*Steel and Composite Structures, Vol. 7, No. 4 (2007) 321-337*
DOI: http://dx.doi.org/10.12989/scs.2007.7.4.321


# Investigation of cold-formed stainless steel non-slender circular hollow section columns

Ehab Ellobody†

*Department of Structural Engineering, Faculty of Engineering, Tanta University, Tanta, Egypt*

Ben Young‡

*Department of Civil Engineering, The University of Hong Kong, Pokfulam Road, Hong Kong*

*(Received September 13, 2006, August 13, 2007)*

**Abstract.** The investigation on the behaviour of cold-formed stainless steel non-slender circular hollow section columns is presented in this paper. The normal strength austenitic stainless steel type 304 and the high strength duplex materials (austenitic-ferritic approximately equivalent to EN 1.4462 and UNS S31803) were considered in this study. The finite element method has been used to carry out the investigation. The columns were compressed between fixed ends at different column lengths. The geometric and material nonlinearities have been included in the finite element analysis. The column strengths and failure modes were predicted. An extensive parametric study was carried out to study the effects of normal and high strength materials on cold-formed stainless steel non-slender circular hollow section columns. The column strengths predicted from the finite element analysis were compared with the design strengths calculated using the American Specification, Australian/New Zealand Standard and European Code for cold-formed stainless steel structures. The numerical results showed that the design rules specified in the American, Australian/New Zealand and European specifications are generally unconservative for the cold-formed stainless steel non-slender circular hollow section columns of normal and high strength materials, except for the short columns and some of the high strength stainless steel columns. Therefore, different values of the imperfection factor and limiting slenderness in the European Code design rules were proposed for cold-formed stainless steel non-slender circular hollow section columns.

**Keywords:** buckling; circular hollow sections; finite element; non-slender; normal strength; high strength; stainless steel; structural design.

## 1. Introduction

Stainless steel structural members have many advantages in terms of high corrosion resistance, ease of construction and maintenance as well as aesthetic appearance. Tests of cold-formed stainless steel columns have been conducted by Rasmussen and Hancock (1993), Talja and Salmi (1995), Rasmussen (2000), Macdonald *et al*. (2000), Young and Hartono (2002), Young and Liu (2003), Gardner and Nethercot (2004a and 2004b), Young and Lui (2005) and Gardner *et al*. (2006). The recent major

†Lecturer, E-mail: ehab_ellobody@tanta.edu.eg
‡Associate Professor, Corresponding author, E-mail: young@hku.hk

research on cold-formed stainless steel structures is summarized by Gardner (2005). Limited test data were found in the literature on fixed-ended cold-formed stainless steel circular hollow section columns. Young and Hartono (2002) conducted a series of tests on fixed-ended cold-formed stainless steel circular hollow section columns. The column test strengths were compared with the design strengths obtained using the American, Australian/New Zealand and European specifications for cold-formed stainless steel structures as well as with the column strengths obtained from the design rules proposed by Rasmussen and Hancock (1993) and Rasmussen and Rondal (1997). It is concluded that the design strengths predicted by the three specifications are generally unconservative for the cold-formed stainless steel circular hollow section columns, while the design strengths predicted by Rasmussen and Hancock (1993), and Rasmussen and Rondal (1997) conservatively predict the column strengths. Young and Hartono (2002) also conducted reliability analysis to evaluate the reliability of these design rules. However, tests of fixed-ended cold-formed stainless steel circular hollow section columns are limited.

The stainless steel material properties are one of the important factors in the finite element analysis. Stainless steel has a rounded stress-strain curve with no distinct yield plateau and low proportional limit stress compared with carbon steel. Gardner and Nethercot (2004c) described numerical modeling of stainless steel hollow sections using ABAQUS program. The nine-node reduced integration shell element with five degrees of freedom per node (S9R5) was used in the finite element models. It was found good agreement between the numerical and test results. Ellobody and Young (2005) developed a numerical model for analyzing fixed-ended cold-formed high strength stainless steel square and rectangular hollow section columns. ABAQUS (2004) program was used in the analysis. The four-node reduced integration shell element (S4R) was used in the finite element model. It was found good agreement between the experimental and numerical results. The column strengths predicted from the finite element analysis were compared with the design strengths calculated using the American (2002), Australian/New Zealand (2001) and European (1996) specifications for cold-formed stainless steel structures. Ellobody and Young (2005) concluded that the three specifications are generally conservative for cold-formed high strength stainless steel square and rectangular hollow section columns, but unconservative for some of the short columns. Young and Ellobody (2006) developed a numerical model to investigate the behaviour of cold-formed normal strength stainless steel of type 304 slender circular hollow section columns. The investigation focused on large diameter-to-thickness ($D/t$) ratios ranged from 100 to 200. The column strengths predicted from the finite element analysis were compared with the design strengths calculated using the American (2002), Australian/New Zealand (2001) and European (1996) for cold-formed stainless steel structures. It is shown that the design strengths obtained using the Australian/New Zealand and European specifications are generally unconservative for the cold-formed stainless steel slender circular hollow section columns, while the American Specification is generally quite conservative. Therefore, a revised design equation has been proposed.

The main objective of this paper is to investigate the behaviour of cold-formed stainless steel non-slender circular hollow section columns of normal and high strength materials using finite element method. The diameter-to-thickness ($D/t$) ratios of the circular hollow sections ranged from 5 to 62.5 were investigated. The finite element program ABAQUS (2004) was used in the analysis. A parametric study was performed to investigate the effects of the normal and high strength stainless steel materials on cold-formed stainless steel non-slender circular hollow section columns. The results obtained from the finite element model were compared with design strengths calculated using the American (2002), Australian/New Zealand (2001) and European (1996) specifications for cold-formed stainless steel structures.

## 2. Summary of experimental investigation

The experimental investigation of cold-formed stainless steel type 304 circular hollow section columns performed by Young and Hartono (2002) provided the experimental ultimate loads of columns compressed between fixed ends. Three series (Series C1, C2 and C3) of circular hollow section columns were tested. The test specimens were cold-rolled from annealed flat strips of type 304 stainless steel. Each specimen was cut to a specified length ($L$) ranging from 550 to 3000 mm. The measured cross-section dimensions of the test specimens are detailed in Young and Hartono (2002). The test Series C1, C2 and C3 had an average measured outer diameter ($D$) of 89.0, 168.7, and 322.8 mm and an average thickness ($t$) of 2.78, 3.34 and 4.32 mm, respectively. The average measured outer diameter-to-thickness ($D/t$) ratio is 32.0, 50.5 and 74.7 for Series C1, C2 and C3, respectively. The test specimens are labeled such that the test series and specimen length could be identified from the label. For example, the label "C1L1000" defines the specimen belonged to test Series C1, and the letter "L" indicates the length of the specimen followed by the nominal column length of the specimen in mm (1000 mm).

The material properties of each series of normal strength stainless steel specimens were determined by tensile coupon tests. The coupons were taken from the untested specimens at 90° from the weld in the longitudinal direction. The coupon dimensions and the tests conformed to the Australian Standard AS 1391 (1991) for the tensile testing of metals using 12.5 mm wide coupons of gauge length 50 mm. The Young's modulus ($E_o$) was measured as 188, 200 and 203 GPa as well as the measured static 0.2% proof stress ($\sigma_{0.2}$) was 268, 285 and 255 MPa for Series C1, C2 and C3, respectively. The measured elongation after fracture ($\varepsilon_f$) based on a gauge length of 50 mm was 58, 56 and 62% for Series C1, C2 and C3, respectively. The Ramberg-Osgood parameter ($n$) that describes the shape of the stress-strain curve (Ramberg and Osgood 1943) was 4, 7 and 5 for Series C1, C2 and C3, respectively. The tensile coupon tests are detailed in Young and Hartono (2002). The material properties of the duplex high strength stainless steel were taken from measurements of the flat portion for rectangular hollow section specimen as detailed in Young and Lui (2005). The specimen had a nominal depth of 160 mm, nominal width of 80 mm and nominal plate thickness of 3 mm. The measured Young's modulus ($E_o$), static 0.2% proof stress ($\sigma_{0.2}$) and Ramberg-Osgood parameter ($n$) were 208 GPa, 536 MPa and 5, respectively.

The initial overall geometric imperfections of the column specimens were measured prior to testing. The average values of overall imperfections at mid-length were 1/1715, 1/3778 and 1/3834 of the specimen length for Series C1, C2 and C3, respectively. The measured overall geometric imperfections for each test specimen are detailed in Young and Hartono (2002). The initial local geometric imperfections of the cold-formed stainless steel circular hollow section column specimens were measured and detailed in Young and Ellobody (2006). A cold-formed stainless steel circular hollow section test specimen of 250 mm in length of Series C1 was used for the measurement of local imperfections. A maximum magnitude of local plate imperfection was 0.089 mm, which is equal to 3.2% of the plate thickness of the specimen belonged to Series C1. The same factor was used to predict the initial local geometric imperfections for Series C2 and C3.

A servo-controlled hydraulic testing machine was used to apply compressive axial force to the column specimens. The fixed-ended bearings were designed to restrain against axis rotations as well as twist rotations and warping. Displacement control was used to allow the tests to be continued in the post-ultimate range. The column tests are detailed in Young and Hartono (2002).

## 3. Summary of finite element modeling

### *3.1 General*

The finite element program ABAQUS (2004) was used to simulate the cold-formed stainless steel circular hollow section columns tested by Young and Hartono (2002). The model used the measured geometry, initial local and overall geometric imperfections and material properties. The 4-noded doubly curved shell elements with reduced integration S4R is used to model the buckling behaviour of fixed-ended cold-formed stainless steel circular hollow section columns. The mesh size used in the model was approximately 10 mm × 10 mm (length by width). Fig. 1 shows the finite element mesh of specimen C1L1000. Following the testing procedures for Series C1, C2 and C3, the ends of the columns were fixed against all degrees of freedom except for the displacement at the loaded end in the direction of the applied load. The nodes other than the two ends were free to translate and rotate in any directions. The load was applied in increments using the modified RIKS method available in the ABAQUS library. The nonlinear geometry parameter (*NLGEOM) was included to deal with the large displacement analysis. The load application and boundary conditions are detailed in Young and Ellobody (2006).

The measured stress-strain curves of Series C1, C2 and C3 were used in the analysis. The material behaviour provided by ABAQUS allows for a multi-linear stress-strain curve to be used. The first part of the multi-linear curve represents the elastic part up to the proportional limit stress with measured Young's modulus, and the Poisson's ratio was taken as 0.3. Since the analysis of post-buckling may involve large inelastic strains, the nominal (engineering) static stress-strain curves were converted to true stress and logarithmic plastic true strain curves.

Both initial local and overall geometric imperfections were found in the column specimens. Hence, superposition of local buckling mode as well as overall buckling mode with measured magnitudes was used in the finite element analysis. These buckling modes were obtained by carrying Eigenvalue analyses of the column with large *D/t* ratio as well as small *D/t* ratio to ensure local and overall buckling occurs, respectively. Only the lowest buckling mode (Eigenmode 1) was obtained from the Eigenvalue analyses. Since all buckling modes predicted by ABAQUS Eigenvalue analysis are generalized to 1.0, the buckling modes were factored by the measured magnitudes of the initial local and overall geometric imperfections. Modeling of initial local and geometric imperfections is detailed in Young and Ellobody (2006).

Previous studies by Gardner (2002), and Ellobody and Young (2005) on cold-formed stainless steel square and rectangular hollow section columns have shown that the effect of residual stresses on the column ultimate load is considered to be small (less than 0.1%). Cold-formed square hollow section is

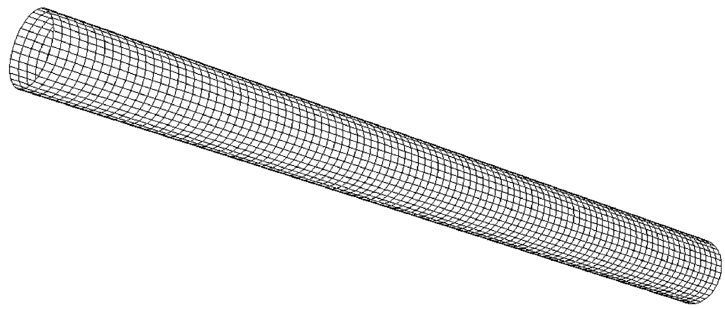

Fig. 1 Finite element mesh of specimen C1L1000

formed by cold-rolling with welds of annealed flat strip into a circular hollow section, and then further rolled into square hollow section. Hence, the effect of residual stresses on the strength and behaviour of cold-formed stainless steel circular hollow section columns would be even smaller than the square and rectangular hollow section columns. Therefore, in order to avoid the complexity of the analysis, the residual stresses were not included in the finite element analysis of cold-formed stainless steel circular hollow section columns.

### 3.2 Verification of finite element model

The verification of the finite element model with test results is detailed in Young and Ellobody (2006). A total of 15 fixed-ended cold-formed normal strength stainless steel circular hollow section columns were analyzed. The results obtained from the finite element analysis were compared with the test results. The comparison of the ultimate loads ($P_{Test}$ and $P_{FE}$) and axial shortening ($e_{Test}$ and $e_{FE}$) at the ultimate loads obtained experimentally and numerically are shown in Table 1. It can be seen that good agreement has been achieved between both results for most of the columns. The experimental failure modes for each of the columns were not reported in Young and Hartono (2002). However, three modes of failure have been observed experimentally and confirmed numerically by the finite element analysis. The failure modes were yielding failure (Y), local buckling (L) and flexural buckling (F). Fig. 2 shows the deformed shape of column specimen C2L2000 observed experimentally and numerically

Table 1 Comparison between test and FE results

| Specimen | Test | | FE | | | Test/FE | |
|---|---|---|---|---|---|---|---|
| | $P_{Test}$ (kN) | $e_{Test}$ (mm) | $P_{FE}$ (kN) | $e_{FE}$ (mm) | Failure mode | $P_{Test}/P_{FE}$ | $e_{Test}/e_{FE}$ |
| C1L550 | 235.2 | 16.88 | 240.5 | 15.41 | Y | 0.98 | 1.10 |
| C1L1000 | 198.4 | 10.26 | 206.8 | 10.89 | Y | 0.96 | 0.94 |
| C1L1500 | 177.4 | 5.77 | 181.8 | 6.54 | F | 0.98 | 0.88 |
| C1L2000 | 165.1 | 4.83 | 167.9 | 5.54 | F | 0.98 | 0.87 |
| C1L2500 | 151.6 | 5.39 | 148.9 | 5.93 | F | 1.02 | 0.91 |
| C1L3000 | 133.4 | 4.99 | 134.5 | 5.41 | F | 0.99 | 0.92 |
| Mean | - | | - | | - | 0.99 | 0.94 |
| COV | - | | - | | - | 0.020 | 0.088 |
| C2L550 | 495.6 | 9.41 | 522.0 | 8.32 | Y | 0.95 | 1.13 |
| C2L1000 | 474.9 | 14.64 | 486.7 | 13.03 | L | 0.98 | 1.12 |
| C2L1500 | 461.0 | 15.92 | 468.9 | 15.25 | L + F | 0.98 | 1.04 |
| C2L2000 | 431.6 | 13.32 | 443.7 | 15.11 | L + F | 0.97 | 0.88 |
| Mean | - | | - | | - | 0.97 | 1.04 |
| COV | - | | - | | - | 0.015 | 0.111 |
| C3L1000 | 1123.9 | 8.05 | 1140.0 | 7.93 | Y | 0.99 | 1.02 |
| C3L1500 | 1119.7 | 14.38 | 1130.0 | 13.12 | Y | 0.99 | 1.10 |
| C3L2000 | 1087.8 | 14.53 | 1100.0 | 14.90 | L | 0.99 | 0.98 |
| C3L2500 | 1045.7 | 19.12 | 1070.0 | 18.05 | L | 0.98 | 1.06 |
| C3L3000 | 1009.5 | 15.64 | 1040.0 | 16.74 | L | 0.97 | 0.93 |
| Mean | - | | - | | - | 0.98 | 1.02 |
| COV | - | | - | | - | 0.009 | 0.065 |

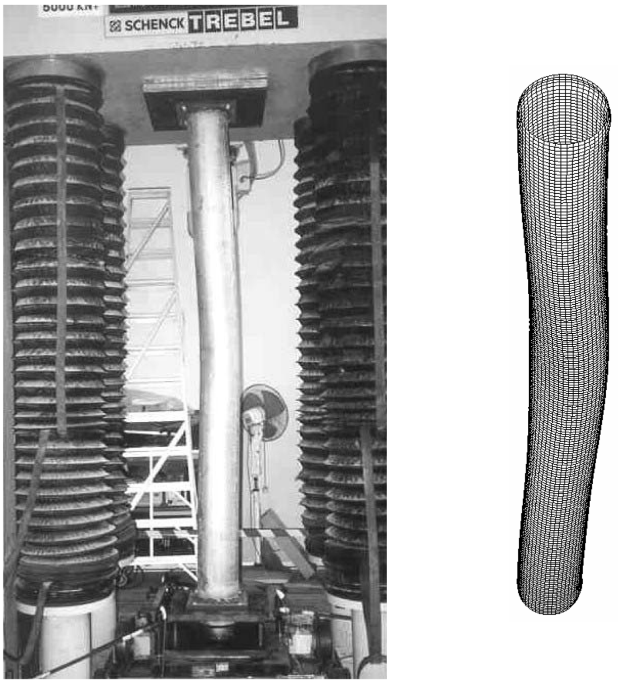


(a) Experimental (b) FE Analysis

Fig. 2 Comparison of experimental and finite element analysis failure modes for specimen C2L2000

using the FE analysis. The column has an outer diameter of 168.7 mm and a length of 2000 mm. The failure modes observed in the test was interaction of local and flexural buckling (L + F). It can be seen that the finite element model accurately predicted the failure modes observed in the test. The applied load versus axial shortening behaviour of the columns was also investigated and detailed in Young and Ellobody (2006). It was shown that good agreement between experimental and finite element results has been achieved.

## 4. Parametric study

A parametric study was carried out to study the effects of the normal and high strength stainless steel materials on cold-formed stainless steel non-slender circular hollow section columns. A total of 70 columns were analyzed using the finite element model. The normal strength stainless steel type 304 columns were analyzed using the measured stress-strain curve of Series C1, and the high strength stainless steel (duplex stainless steel that is approximately equivalent to EN 1.4462 and UNS S31803) columns were analyzed using the measured stress-strain curve as described in the Section of experimental investigation. The columns are labeled such that the outer diameter, the plate thickness and column length could be identified from the label. For example, the label “D50T2.5L1000” defines the circular hollow section column having an outer diameter indicated by the letter “D” followed by the value of the outer diameter in mm (50 mm), the letter “T” defines the plate thickness of the column followed by the value of the plate thickness in mm (2.5 mm), and the letter “L” indicates the length of the column

Table 2 Specimen dimensions of parametric study

| Specimen | *D* (mm) | *t* (mm) | *D/t* | *L* (mm) |
|---|---|---|---|---|
| D50T2.5L500 | 50 | 2.5 | 20.0 | 500 |
| D50T2.5L1000 | 50 | 2.5 | 20.0 | 1000 |
| D50T2.5L1500 | 50 | 2.5 | 20.0 | 1500 |
| D50T2.5L2000 | 50 | 2.5 | 20.0 | 2000 |
| D50T2.5L2500 | 50 | 2.5 | 20.0 | 2500 |
| D50T2.5L3000 | 50 | 2.5 | 20.0 | 3000 |
| D50T2.5L3500 | 50 | 2.5 | 20.0 | 3500 |
| D50T10L500 | 50 | 10 | 5.0 | 500 |
| D50T10L1000 | 50 | 10 | 5.0 | 1000 |
| D50T10L1500 | 50 | 10 | 5.0 | 1500 |
| D50T10L2000 | 50 | 10 | 5.0 | 2000 |
| D50T10L2500 | 50 | 10 | 5.0 | 2500 |
| D50T10L3000 | 50 | 10 | 5.0 | 3000 |
| D50T10L3500 | 50 | 10 | 5.0 | 3500 |
| D75T1.2L500 | 75 | 1.2 | 62.5 | 500 |
| D75T1.2L1000 | 75 | 1.2 | 62.5 | 1000 |
| D75T1.2L1500 | 75 | 1.2 | 62.5 | 1500 |
| D75T1.2L2000 | 75 | 1.2 | 62.5 | 2000 |
| D75T1.2L2500 | 75 | 1.2 | 62.5 | 2500 |
| D75T1.2L3000 | 75 | 1.2 | 62.5 | 3000 |
| D75T1.2L3500 | 75 | 1.2 | 62.5 | 3500 |
| D75T7.5L500 | 75 | 7.5 | 10.0 | 500 |
| D75T7.5L1000 | 75 | 7.5 | 10.0 | 1000 |
| D75T7.5L1500 | 75 | 7.5 | 10.0 | 1500 |
| D75T7.5L2000 | 75 | 7.5 | 10.0 | 2000 |
| D75T7.5L2500 | 75 | 7.5 | 10.0 | 2500 |
| D75T7.5L3000 | 75 | 7.5 | 10.0 | 3000 |
| D75T7.5L3500 | 75 | 7.5 | 10.0 | 3500 |
| D100T2.5L500 | 100 | 2.5 | 40.0 | 500 |
| D100T2.5L1000 | 100 | 2.5 | 40.0 | 1000 |
| D100T2.5L1500 | 100 | 2.5 | 40.0 | 1500 |
| D100T2.5L2000 | 100 | 2.5 | 40.0 | 2000 |
| D100T2.5L2500 | 100 | 2.5 | 40.0 | 2500 |
| D100T2.5L3000 | 100 | 2.5 | 40.0 | 3000 |
| D100T2.5L3500 | 100 | 2.5 | 40.0 | 3500 |

followed by the column length in mm (1000 mm). The columns are divided into five series of circular hollow sections (Series D50T2.5, D50T10, D75T1.2, D75T7.5 and D100T2.5) having outer diameters of 50, 50, 75, 75 and 100 mm, and plate thickness of 2.5, 10, 1.2, 7.5 and 2.5 mm, respectively. The Series D50T2.5, D50T10, D75T1.2, D75T7.5 and D100T2.5 had the outer diameter-to-thickness ratio (*D/t*) of 20, 5, 62.5, 10 and 40, respectively, covering non-slender sections. Each series of columns

Table 3 Summary of parametric study results

| Specimen | Normal strength (Stainless steel type 304) | | | High strength (Duplex stainless steel) | | |
|---|---|---|---|---|---|---|
| | $P_{FE}$ (kN) | $e_{FE}$ (mm) | Failure mode | $P_{FE}$ (kN) | $e_{FE}$ (mm) | Failure mode |
| D50T2.5L500 | 112.6 | 8.54 | Y | 213.2 | 6.69 | Y |
| D50T2.5L1000 | 89.6 | 4.62 | F | 205.3 | 6.50 | Y |
| D50T2.5L1500 | 71.3 | 3.57 | F | 167.8 | 3.80 | F |
| D50T2.5L2000 | 60.7 | 2.88 | F | 139.0 | 3.61 | F |
| D50T2.5L2500 | 58.0 | 2.11 | F | 111.4 | 3.60 | F |
| D50T2.5L3000 | 53.2 | 2.32 | F | 82.1 | 3.40 | F |
| D50T2.5L3500 | 46.8 | 2.42 | F | 55.5 | 2.61 | F |
| D50T10L500 | 364.0 | 5.50 | Y | 706.4 | 5.97 | Y |
| D50T10L1000 | 275.7 | 3.39 | F | 650.5 | 5.85 | F |
| D50T10L1500 | 221.7 | 2.74 | F | 488.8 | 3.41 | F |
| D50T10L2000 | 203.0 | 1.74 | F | 380.0 | 3.23 | F |
| D50T10L2500 | 180.6 | 1.95 | F | 272.2 | 2.71 | F |
| D50T10L3000 | 155.6 | 2.06 | F | 190.2 | 2.31 | F |
| D50T10L3500 | 126.2 | 2.07 | F | 139.9 | 2.03 | F |
| D75T1.2L500 | 86.7 | 6.84 | Y | 164.4 | 6.26 | Y |
| D75T1.2L1000 | 76.0 | 7.06 | Y | 153.4 | 6.97 | Y |
| D75T1.2L1500 | 67.4 | 7.05 | F | 135.0 | 4.62 | L |
| D75T1.2L2000 | 57.1 | 5.35 | F | 118.0 | 4.07 | F |
| D75T1.2L2500 | 50.9 | 5.00 | F | 108.0 | 3.82 | F |
| D75T1.2L3000 | 45.7 | 4.58 | F | 97.0 | 3.64 | F |
| D75T1.2L3500 | 44.9 | 3.07 | F | 86.0 | 3.49 | F |
| D75T7.5L500 | 539.0 | 11.80 | Y | 935.0 | 9.59 | Y |
| D75T7.5L1000 | 430.0 | 6.70 | Y | 859.0 | 6.59 | Y |
| D75T7.5L1500 | 375.0 | 5.56 | F | 740.0 | 5.44 | F |
| D75T7.5L2000 | 314.5 | 4.87 | F | 644.0 | 4.73 | F |
| D75T7.5L2500 | 278.3 | 4.52 | F | 580.0 | 4.49 | F |
| D75T7.5L3000 | 249.1 | 3.97 | F | 520.0 | 4.31 | F |
| D75T7.5L3500 | 244.5 | 2.87 | F | 460.0 | 4.26 | F |
| D100T2.5L500 | 264.6 | 14.97 | Y | 454.0 | 7.41 | Y |
| D100T2.5L1000 | 229.6 | 12.83 | Y | 432.0 | 7.12 | Y |
| D100T2.5L1500 | 203.2 | 9.76 | F | 398.0 | 7.10 | F |
| D100T2.5L2000 | 185.1 | 9.29 | F | 355.0 | 6.20 | F |
| D100T2.5L2500 | 161.3 | 7.34 | F | 325.0 | 6.06 | F |
| D100T2.5L3000 | 147.1 | 6.82 | F | 304.7 | 5.82 | F |
| D100T2.5L3500 | 136.3 | 6.50 | F | 290.0 | 5.71 | F |

consists of seven column lengths of 500, 1000, 1500, 2000, 2500, 3000 and 3500 mm. A summary of the specimen dimensions of the parametric study is presented in Table 2. The longest specimen lengths produced $l_e/r$ ratio of 104.0, 120.0, 67.0, 72.9 and 50.8 for Series D50T2.5, D50T10, D75T1.2, D75T7.5 and D100T2.5, respectively, where $l_e$ ($l_e = L/2$) is the effective length and $r$ is the radius of gyration. The maximum initial local geometric imperfection magnitude was taken as the measured value of test Series C1 that is equal to 3.2% of the plate thickness. The initial overall geometric imperfection magnitude was taken as the average of the measured overall imperfections of the test Series C1 which is equal to $L$ / 1715, where $L$ is the column length. A summary of the parametric study results is presented in Table 3. The ultimate loads ($P_{FE}$), axial shortening ($e_{FE}$) at the ultimate loads and failure modes are given in Table 3. As for the columns having normal strength stainless steel type 304, the yielding failure mode (Y) was obtained for the short column specimens of Series D50T2.5 and D50T10 with the length of 500 mm as well as obtained for the columns of Series D75T1.2, D75T7.5 and D100T2.5 with the lengths of 500 and 1000 mm. The pure flexural buckling mode was predicted for the rest of the columns. Similar failure modes were observed for the columns having high strength stainless steel (duplex stainless steel), except for the columns D50T2.5L1000 and D75T1.2L1000 where yielding and local buckling were predicted, respectively. The ultimate loads obtained from the parametric study were also plotted against the effective length $l_e$ ($l_e = L / 2$) as shown in Figs. 3 and 4.

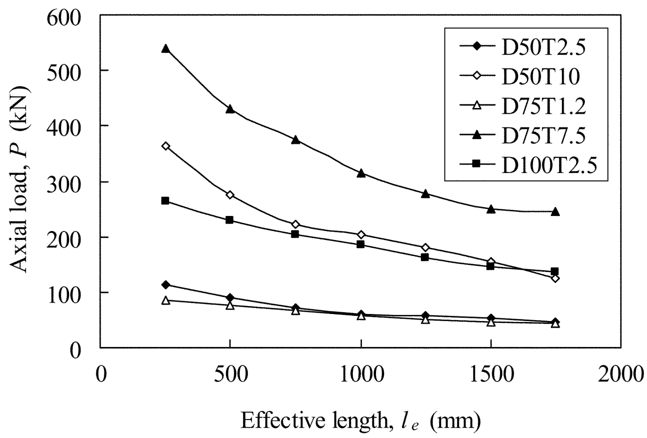


Fig. 3 FE strengths and effective length relationships for columns using normal strength stainless steel

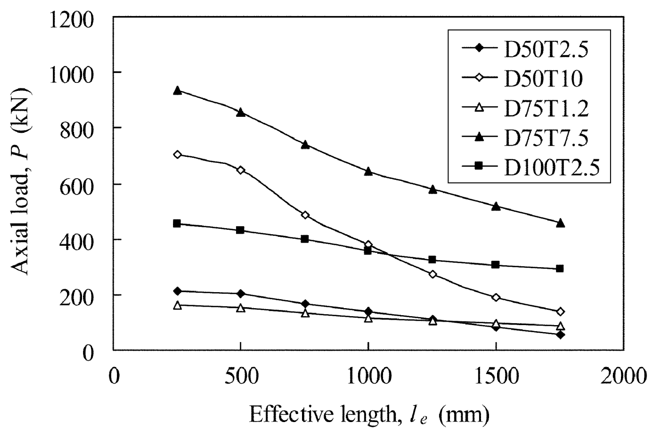


Fig. 4 FE strengths and effective length relationships for columns using high strength stainless steel

## 5. Comparison of column strengths

The column strengths predicted from the parametric study were compared with the unfactored design strengths calculated using the American (ASCE, 2002), Australian/New Zealand (AS/NZS, 2001) and European (EC3, 1996) specifications for cold-formed stainless steel structures. The measured material properties obtained from the tensile coupon test of Series C1 were used to predict the design strengths for the columns of normal stainless steel type 304, while, the measured material properties obtained from the tensile coupon test of the high strength stainless steel as detailed in the experimental investigation section were used to predict the design strengths for the columns of high strength stainless steel. The design rules specified in the ASCE Specification are based on the Euler column strength that requires the calculation of tangent modulus ($E_t$) using an iterative design procedure. The design rules specified in the EC3 Code are based on the Perry curve that needs only the initial Young's modulus ($E_o$) and a number of parameters to calculate the design stress. The design rules specified in the AS/NZS Standard adopts either the Euler column strength or the Perry curve and the latter is used in this paper. The fixed-ended columns were designed as concentrically loaded compression members and the effective length ($l_e$) was taken as one-half of the column length ($l_e = L/2$) as recommended by Young and Rasmussen (1998).

The tangent modulus ($E_t$) required for the calculation of the ASCE design strengths was determined using Eq. (B-2) in Appendix B of the specification. The factors $\alpha$, $\beta$, $\lambda_o$ and $\lambda_1$, required for the calculation of the AS/NZS design strengths were calculated from the equations proposed by Rasmussen and Rondal (1997) depending on the ($\sigma_{0.2}/E_o$) ratio and the Ramberg-Osgood parameter $n$ obtained from the tensile coupon test of Series C1. The calculated values were 1.483, 0.231, 0.608 and 0.272 for $\alpha$, $\beta$, $\lambda_o$ and $\lambda_1$, respectively. The values of the imperfection factor and limiting slenderness required for the calculation of the EC3 design strengths were obtained from Table 5.2 of the Code.

According to the EC3, the effective area ($A_e$) is taken as the full area ($A$) for Class 1 ($D/t \le 50\varepsilon^2$), Class 2 ($D/t\ 70 \le \varepsilon^2$) and Class 3 ($D/t\ 90 \le \varepsilon^2$) cross-sections, where $\varepsilon$ is calculated as ($\varepsilon = \sqrt{\frac{235}{F_y}\frac{E_o}{210000}}$). Although the aim of this study is to investigate the behaviour of non-slender circular hollow sections, Series D75T1.2 and D100T2.5 are classified as slender circular hollow

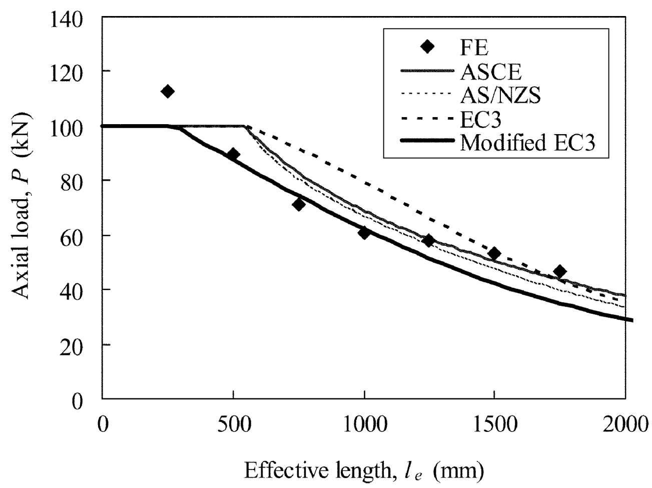


Fig. 5 Comparison of FE strengths with design strengths for Series D50T2.5 using normal strength stainless steel

sections if the high strength stainless steel material is used, while it is considered as non-slender sections if the normal strength stainless steel material is used.

Figs. 5-9 show a comparison between the strengths of the columns having normal strength stainless steel type 304 obtained from the finite element analysis with the nominal (unfactored) design strengths obtained using the American Specification (2002), Australian/New Zealand Standard (2001) and European Code (1996). The column strengths are shown on the vertical axis of Figs. 5-9, while the horizontal axis is plotted as the effective length ($l_e$) that is assumed equal to one-half of the column length. It can be seen that the ASCE, AS/NZS and EC3 specifications are generally unconservative for the cold-formed stainless steel circular hollow section columns, except for column lengths of 3000 and 3500 mm of Series D50T2.5 and D50T10 having an outer diameter of 50 mm and outer diameter-to-thickness ratio ($D/t$) of 20 and 5, respectively. The ASCE, AS/NZS and EC3 specifications underestimated the

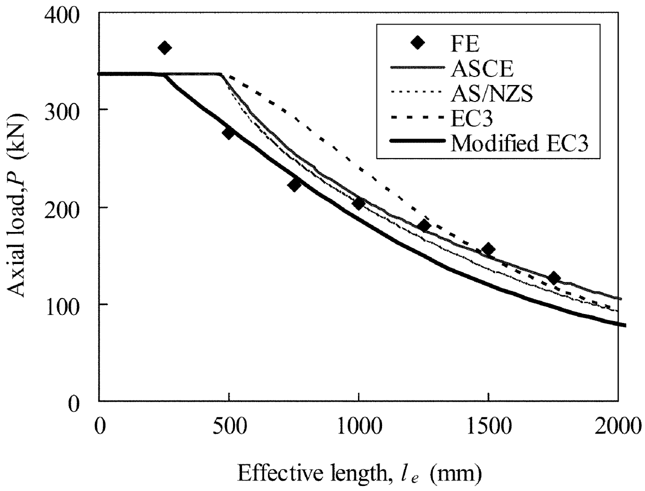


Fig. 6 Comparison of FE strengths with design strengths for Series D50T10 using normal strength stainless steel

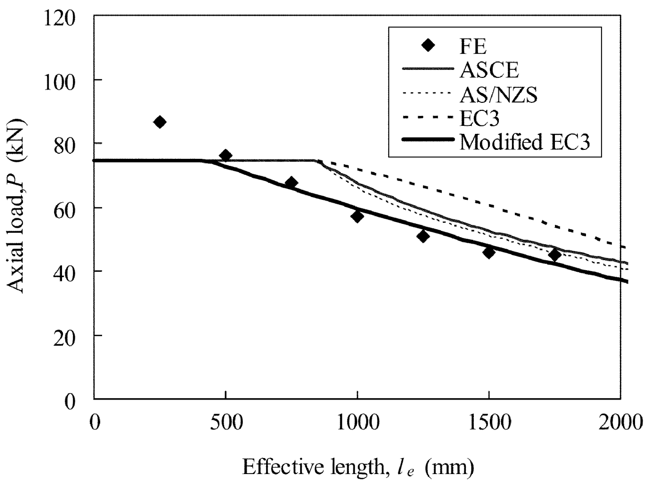


Fig. 7 Comparison of FE strengths with design strengths for Series D75T1.2 using normal strength stainless steel

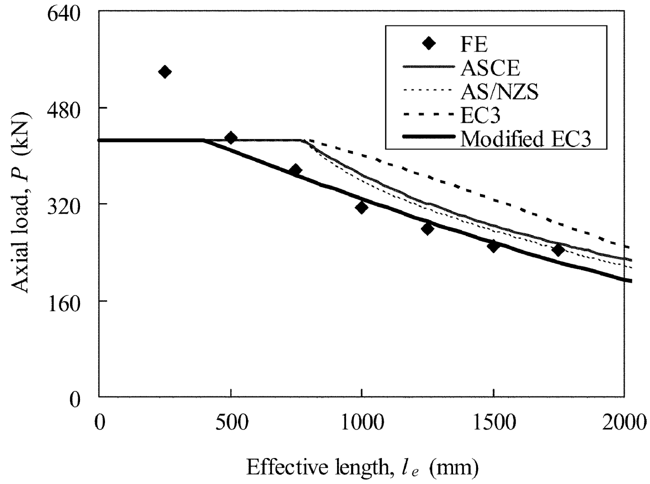


Fig. 8 Comparison of FE strengths with design strengths for Series D75T7.5 using normal strength stainless steel

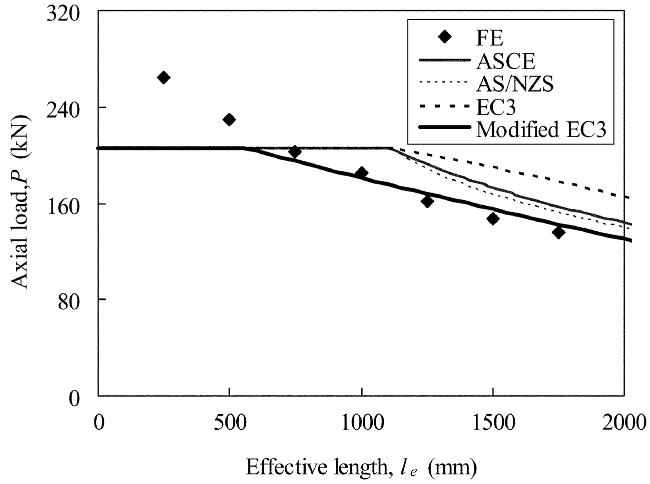


Fig. 9 Comparison of FE strengths with design strengths for Series D100T2.5 using normal strength stainless steel

column strengths of short columns of length 500 mm for all series as well as columns of length 1000 mm of Series D75T1.2, D75T7.5 and D100T2.5.

Figs. 10-14 show a comparison between the strengths of the columns having high strength stainless steel (duplex stainless steel) obtained from the finite element analysis with the nominal design strengths. It can be seen that the ASCE and AS/NZS accurately predict the design strengths of the columns in Series D50T2.5 and D50T10, except for some long columns, while the EC3 is generally conservative, as shown in Figs. 10 and 11. The ASCE and AS/NZS specifications are generally unconservative for the columns in Series D75T1.2, D75T7.5 and D100T2.5, while the EC3 is generally conservative, as shown in Figs. 12-14.

The strength (normal and high strength materials) of stainless steel plays an important role on the behaviour of cold-formed stainless steel non-slender circular hollow section columns. It could affect the failure mode of the columns. This has been found in specimen D75T1.2L1500 that failed

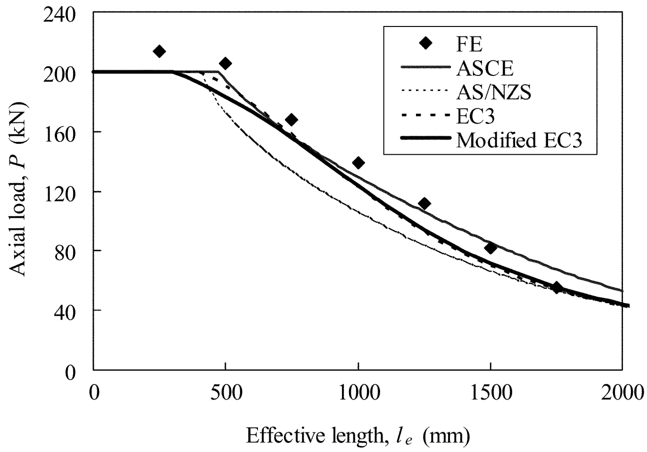


Fig. 10 Comparison of FE strengths with design strengths for Series D50T2.5 using high strength stainless steel

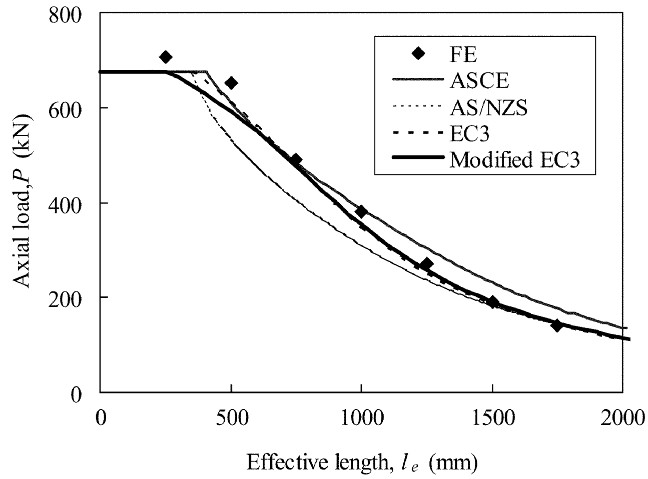


Fig. 11 Comparison of FE strengths with design strengths for Series D50T10 using high strength stainless steel

by local buckling when high strength stainless steel material was used rather than flexural buckling when normal strength stainless steel material was used, as shown in Table 3. Fig. 15 shows the different failure modes of specimens D75T1.2L1500 for normal and high strength stainless steel materials.

## 6. Design recommendations

The following recommendations are made for the design of cold-formed stainless steel non-slender circular hollow section columns. The comparison of the column strengths obtained from the parametric study and the design strengths has shown that the design rules specified in the American, Australian/New Zealand and European specifications are generally unconservative for the cold-formed normal and high strengths stainless steel non-slender circular hollow section columns, except for the short columns

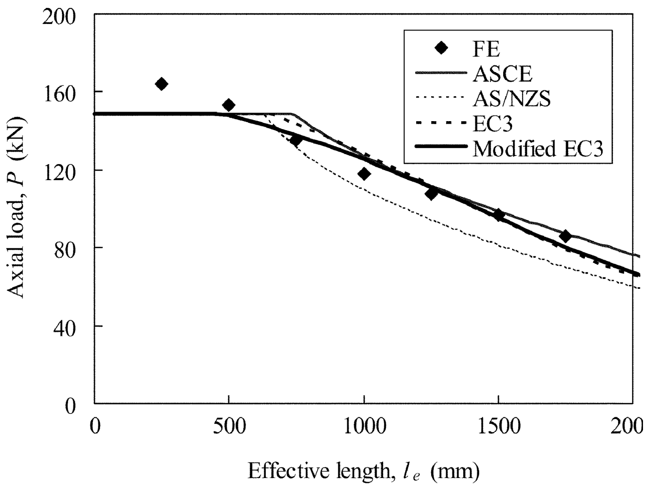


Fig. 12 Comparison of FE strengths with design strengths for Series D75T1.2 using high strength stainless steel

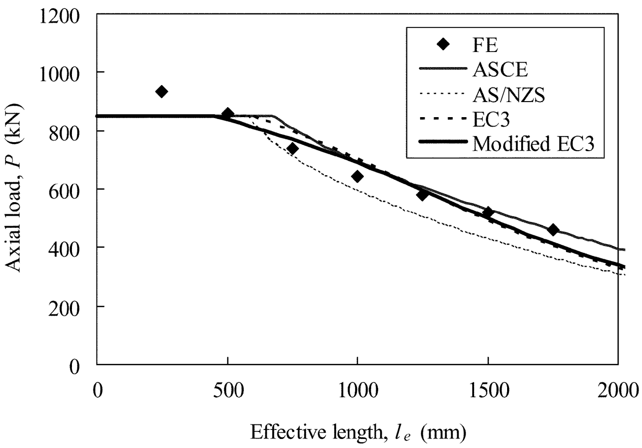


Fig. 13 Comparison of FE strengths with design strengths for Series D75T7.5 using high strength stainless steel

and some high strength stainless steel columns. Therefore, different imperfection factors and limiting slenderness in the European Code design rules were proposed for non-slender circular hollow section columns.

In this study, it is found that the use of the imperfection factor $\alpha = 0.8$ and limiting slenderness $\bar{\lambda}_o = 0.2$ rather than that obtained from Table 5.2 of the EC3 Code ($a = 0.49$ and $\bar{\lambda}_o = 0.4$) provide more accurate results for the cold-formed normal strength stainless steel non-slender circular hollow section columns. On the other hand, the use of the imperfection factor $\alpha = 0.4$ and limiting slenderness $\bar{\lambda}_o = 0.3$ provide more accurate results than the values given by the EC3 Code for the cold-formed high strength stainless steel non-slender circular hollow section columns. Generally, these recommendations lead to conservative design as shown in Figs. 5-14.

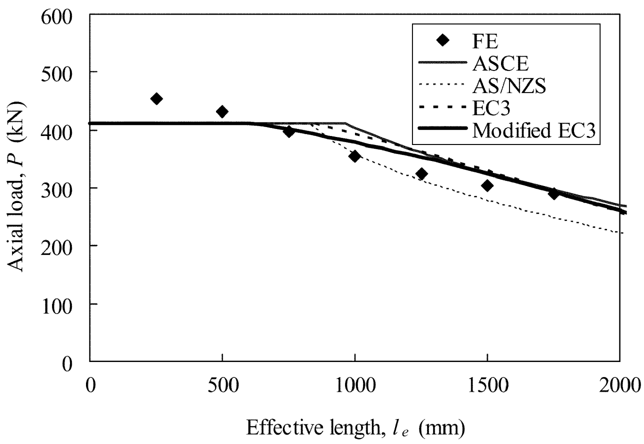


Fig. 14 Comparison of FE strengths with design strengths for Series D100T2.5 using high strength stainless steel

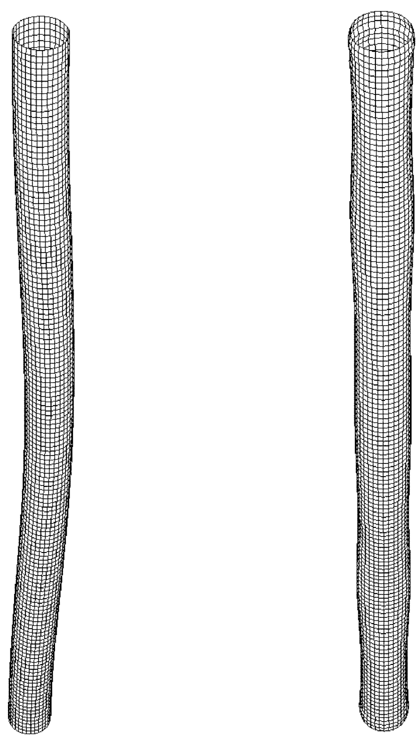

(a) Flexural buckling (F) of normal strength stainless steel specimen

(b) Local buckling (L) of high strength stainless steel specimen

Fig. 15 FE failure modes of specimen D75T1.2L1500 using normal and high strengths stainless steel

## 7. Conclusions

The investigation on the behaviour of cold-formed normal and high strengths stainless steel non-slender circular hollow section columns has been presented. A nonlinear finite element analysis has been conducted. The initial local and overall geometric imperfections as well as nonlinear material properties of the normal and high strengths stainless steel circular hollow section columns have been included in the finite element analysis. The column strengths and failure modes have been predicted and compared well with the experimental results. Parametric study was performed to study the effects of normal and high strength materials on cold-formed stainless steel non-slender circular hollow section columns.

The results of the parametric study showed that the design rules specified in the American, Australian/New Zealand and European specifications are generally unconservative for the cold-formed normal and high strength stainless steel non-slender circular hollow section columns, except for the short columns and some of the high strength stainless steel columns. Therefore, new values of the imperfection factor and limiting slenderness in the European Code are proposed for cold-formed normal and high strengths stainless steel non-slender circular hollow section columns. It is found that the use of the imperfection factor of 0.8 and limiting slenderness of 0.2 provide more accurate predictions than the values given by the European Code for the cold-formed normal strength stainless steel non-slender circular hollow section columns. On the other hand, the use of the imperfection factor of 0.4 and limiting slenderness of 0.3 provide accurate predictions for the cold-formed high strength stainless steel non-slender circular hollow section columns.

## References


ABAQUS Standard User's Manual (2004), Hibbitt, Karlsson and Sorensen, Inc. Vol. 1, 2 and 3, Version 6.4, USA.

ASCE (2002), *Specification for the design of cold-formed stainless steel structural members*. American Society of Civil Engineers, SEI/ASCE-8-02, Reston, Virginia.

AS (1991), *Methods for tensile testing of metals*. Australian Standard, AS 1391 – 1991, Standards Association of Australia, Sydney, Australia.

AS/NZS (2001), *Cold-formed Stainless Steel Structures*. Australian/New Zealand Standard, AS/NZS 4673:2001, Standards Australia, Sydney, Australia.

EC3 (1996), *Eurocode 3: Design of steel structures – Part 1.4: General rules – Supplementary rules for stainless steels*. European Committee for Standardization, ENV 1993-1-4, CEN, Brussels.

Ellobody, E. and Young, B. (2005), "Structural performance of cold-formed high strength stainless steel columns", *J. Constr. Steel Res.*, **61**(12), 1631-1649.

Gardner, L. (2002), "A new approach to structural stainless steel design", PhD thesis, Department of Civil and Environmental Engineering, Imperial College of Science, Technology and Medicine, London.

Gardner, L. (2005), "The use of stainless steel in structures", *Progress in Structural Engineering and Materials*, **7**(2), 45-55.

Gardner, L. and Nethercot, D. A. (2004a), "Experiments on stainless steel hollow sections – Part 1: Material and cross-sectional behaviour", *J. Constr. Steel Res.*, **60**(9), 1291-1318.

Gardner, L. and Nethercot, D.A. (2004b), "Experiments on stainless steel hollow sections – Part 2: Member behaviour of columns and beams", *J. Constr. Steel Res.*, **60**(9), 1319-1332.

Gardner, L. and Nethercot, D. A. (2004c), "Numerical modeling of stainless steel structural components - A consistent approach", *J. Struct. Eng.*, ASCE, **130**(10), 1586-1601.

Gardner, L., Talja, A. and Baddoo, N. R. (2006), "Structural design of high-strength austenitic stainless steel", *Thin-Walled Struct.*, **44**(5), 517-528.

Macdonald, M., Rhodes, J. and Taylor, G. T. (2000), "Mechanical properties of stainless steel lipped channels", *Proceedings of the Fifteenth International Specialty Conference on Cold-formed Steel Structures*, Eds R. A. LaBoube and W. W. Yu, St. Louis, University of Missouri-Rolla, Mo., USA, 673-686.

Ramberg, W. and Osgood, W.R. (1943), "Description of stress strain curves by three parameters", *Tech. Note No*

*902,* National Advisory committee for Aeronautics, Washington, D.C.
Rasmussen, K. J. R. (2000), "Recent research on stainless steel tubular structures", *J. Constr. Steel Res.*, **54**, 75-88.
Rasmussen, K. J. R. and Hancock, G. J. (1993), "Design of cold-formed stainless steel tubular members. I: Columns", *J. Struct. Eng.*, ASCE, **119**(8), 2349-2367.
Rasmussen, K.J.R. and Rondal, J. (1997), "Strength curves for metal columns", *J. Struct. Eng.*, ASCE, **123**(6), 721-728.
Talja, A. and Salmi, P. (1995), "Design of stainless steel RHS beams, columns and beam-columns", VTT *Research Notes* 1619, Technical Research Centre of Finland, Espoo.
Young, B. and Ellobody, E. (2006), "Column design of cold-formed stainless steel slender circular hollow sections", *Steel Compos. Struct.*, **6**(4), 285-302.
Young, B. and Hartono, W. (2002), "Compression tests of stainless steel tubular members", *J. Struct. Eng.*, ASCE, **128**(6), 754-761.
Young, B. and Liu, Y. (2003), "Experimental investigation of cold-formed stainless steel columns", *J. Struct. Eng.*, ASCE, **129**(2), 169-176.
Young, B. and Lui, W. M. (2005), "Behavior of cold-formed high strength stainless steel sections", *J. Struct. Eng.*, ASCE, **131**(11), 1738-1745.
Young, B. and Rasmussen, K. J. R. (1998), "Tests of fixed-ended plain channel columns", *J. Struct. Eng.*, ASCE, **124**(2), 131-139.

## Notation

The following symbols are used in this paper:

$A$ : gross cross-section area;
$A_e$ : effective cross-section area;
$D$ : outer diameter;
$E_o$ : Young's modulus;
$E_t$ : tangent modulus;
$e_{FE}$ : axial shortening from finite element analysis at ultimate load;
$e_{Test}$ : axial shortening from tests at ultimate load;
$K_c$ : factor used in design specifications to calculate effective area;
$L$ : length of column specimen;
$l_e$ : column effective length;
$n$ : exponent in Ramberg-Osgood expression;
$P$ : axial compressive load;
$P_{FE}$ : finite element ultimate load;
$P_{Test}$ : test ultimate load;
$r$ : radius of gyration;
$t$ : plate thickness of specimen;
$\varepsilon$ : strain;
$\varepsilon_f$ : elongation (tensile strain) after fracture based on gauge length of 50mm;
$\varepsilon_{true}^{pl}$ : plastic true strain;
$\alpha$ : parameter;
$\beta$ : parameter;
$\lambda_o$ : parameter;
$\lambda_1$ : parameter;
$\lambda_c$ : non-dimensional slenderness;
$\sigma$ : stress;
$\sigma_{0.2}$ : static 0.2% tensile proof stress; and
$\sigma_{true}$ : true stress
*CC*